ARMY RESEARCH LABORATORY

Optical Turbulence Effects on Ground to Satellite Microwave Refractivity

by Arnold Tunick

ARL-MR-0640 **May 2006**

NOTICES

Disclaimers

The findings in this report are not to be construed as an official Department of the Army position unless so designated by other authorized documents.

Citation of manufacturer's or trade names does not constitute an official endorsement or approval of the use thereof.

Destroy this report when it is no longer needed. Do not return it to the originator.

Army Research Laboratory
Adelphi, MD 20783-1197

ARL-MR-0640 **May 2006**

Optical Turbulence Effects on Ground to Satellite Microwave Refractivity

Arnold Tunick
Computational and Information Sciences Directorate, ARL

REPORT DOCUMENTATION PAGE

Form Approved
OMB No. 0704-0188

1. REPORT DATE *(DD-MM-YYYY)*	2. REPORT TYPE	3. DATES COVERED (From - To)
May 2006	Final	February 2006 to April 2006

4. TITLE AND SUBTITLE
Optical Turbulence Effects on Ground to Satellite Microwave Refractivity

5a. CONTRACT NUMBER

5b. GRANT NUMBER

5c. PROGRAM ELEMENT NUMBER

6. AUTHOR(S)
Arnold Tunick

5d. PROJECT NUMBER

5e. TASK NUMBER

5f. WORK UNIT NUMBER

7. PERFORMING ORGANIZATION NAME(S) AND ADDRESS(ES)
U.S. Army Research Laboratory
ATTN: AMSRD-ARL-CI-CN
2800 Powder Mill Road
Adelphi, MD 20783-1197

8. PERFORMING ORGANIZATION REPORT NUMBER
ARL-MR-0640

9. SPONSORING/MONITORING AGENCY NAME(S) AND ADDRESS(ES)
U.S. Army Research Laboratory
2800 Powder Mill Road
Adelphi, MD 20783-1197

10. SPONSOR/MONITOR'S ACRONYM(S)

11. SPONSOR/MONITOR'S REPORT NUMBER(S)

12. DISTRIBUTION/AVAILABILITY STATEMENT
Approved for public release; distribution unlimited.

13. SUPPLEMENTARY NOTES

14. ABSTRACT

Due to the increased use of laser and microwave ground-to-satellite communications the need for reliable optical turbulence information is growing. Optical turbulence information is important because it describes an atmospheric effect that can degrade the performance of electromagnetic systems and sensors, e.g., free-space optical and microwave communications and infrared imaging. A quantitative measure of the intensity of optical turbulence is the refractive index structure parameter, *Cn2*. A critical analysis of selected past research on optical turbulence in diverse microclimate environments indicates that the magnitude of *Cn2* generally increases with increasing wavelength. This is because the overall contribution to *Cn2* due to moisture (i.e., humidity gradient) effects significantly increases with increasing wavelength. As an example, the values for near-millimeter wave *Cn2* can be larger by an order of magnitude or more than ones in the infrared, which are mainly dependent on temperature structure. Hence, this paper provides a brief review of temperature and humidity effects on microwave *Cn2*, to include key computational algorithms and comprehensive reference citations. We anticipate that this work will be useful and informative to those interested in the design and performance of earth and space communication systems.

15. SUBJECT TERMS
Radio frequency communications, Cn2, temperature and humidity effects

16. SECURITY CLASSIFICATION OF:			17. LIMITATION OF ABSTRACT	18. NUMBER OF PAGES	19a. NAME OF RESPONSIBLE PERSON
a. REPORT	b. ABSTRACT	c. THIS PAGE			Arnold Tunick
Unclassified	Unclassified	Unclassified	UL	30	19b. TELEPHONE NUMBER (*Include area code*) (301) 394-1765

Standard Form 298 (Rev. 8/98)
Prescribed by ANSI Std. Z39.18

Contents

List of Figures

List of Tables

Acknowledgments

The author extends thanks to Ronald Meyers of the U.S. Army Research Laboratory for offering many helpful comments on this study.

INTENTIONALLY LEFT BLANK.

1. Introduction

Optical turbulence is an atmospheric effect that acts on the propagation of light waves to distort electro-magnetic propagation paths and intensity. It is brought about by fluctuations in the refractive index in air, i.e., air density, which affects the speed at which light wave-fronts propagate. Atmospheric refractions of electro-magnetic energy can cause spatial and temporal (intensity) variations in transmitted signals (Chiba, 1971; Fried, 1967; Ishimaru, 1978; and Parry, 1981). In turn, these effects can significantly degrade (blur, shimmer, and distort) infrared images or increase transmission bit error rates in free-space laser and microwave communication systems. In an experiment to establish the first known optical communication link using lasers (from a mountaintop observatory) to a low earth orbiting satellite, Wilson et al. (1997) commented, "If left uncompensated (i.e., no adaptive beam forming or beam steering techniques applied) these [optical turbulence related] effects would cause fades and surges in the uplink signal, and result in high bit errors in the uplink communications data stream." Similarly, for satellite communication systems at frequencies above 10 GHz, Vasseur (1999) commented that optical turbulence can bring about random fades and enhancements of received signals, which could impair the overall availability of the system and interfere with tracking and fade mitigation applications. In contrast, Vander Vorst et al. (1997) contended that the most significant effect on satellite communication links (at frequencies above 10 GHz) was tropospheric scintillation due to turbulence in clouds, in particular, that brought about by the entrainment process at the top of cumulus clouds, for example. Other signal degrading effects discussed in the paper by Vander Vorst et al. (1997) were those due to depolarization induced by rain and ice crystals and interference between space and terrestrial radio communication links sharing the same frequency bands.

Nevertheless, many research studies focusing on optical turbulence and its influences on electro-magnetic wave propagation in the atmosphere have highlighted measured and modeled estimates for the refractive index structure parameter, *Cn2*. As outlined in the following sections, *Cn2* is a quantitative measure of the intensity of optical turbulence that can be derived for visible, infrared, millimeter, and radio wavelengths. However, it is generally agreed that path-integrated values of *Cn2* are more useful than values of *Cn*2 at several discrete points (Kopeika, 1998). Calculation of the angle-of-arrival fluctuation variance, $\left\langle \sigma_A^2 \right\rangle$, and the log-intensity (or log-amplitude) variance of transmitted electromagnetic signals, $\left\langle \sigma_x^2 \right\rangle$, contain this type of information (Beland, 1993). Thus, improving future optical turbulence calculations will provide better estimates of *Cn2* along more complex optical lines-of-site. This will result in better estimates of displacement, $\left\langle \sigma_A^2 \right\rangle$, and intensity fluctuations, $\left\langle \sigma_x^2 \right\rangle$, which are just two examples of the kinds improved work product that may

contribute important information on the performance of many electro-optical systems and sensors (Tunick, 2005).

2. Microwave *Cn2* Data and Models

Values of visible and infrared wavelength *Cn2* in the atmospheric surface layer near the ground have been generally observed to range from about 10^{-12} to 10^{-16} $m^{-2/3}$ (Kallistratova and Timanovskiy, 1971; Darizhapov et al., 1988). High values of visible or infrared *Cn2*, 10^{-12} $m^{-2/3}$ or greater, usually indicate a highly turbulent atmosphere and the potential for considerable visual blurring (e.g., the wavy lines one might encounter looking out over a hot paved road). At lower values of this *Cn2*, 10^{-16} to 10^{-15} $m^{-2/3}$, atmospheric optical turbulence might be considered negligible over shorter (≤ 2 km) optical paths although there could be other image-degrading effects due to aerosols, precipitation, fog, or smoke. In contrast, Tunick and Rachele (1991) found that model estimates of millimeter and radio wave *Cn2* were equal to or greater than 10^{-11} $m^{-2/3}$ over wet and dry soils. They and others [see Tunick (2002) for a critical analysis of selected past research on optical turbulence in diverse microclimate environments] have suggested that the magnitude of *Cn2* generally increases with increasing wavelength. This is because the overall contribution to *Cn2* due to moisture (i.e., humidity gradient) effects significantly increases with increasing wavelength. As an example, Bohlander et al. (1985) commented that the values for near-millimeter wave *Cn2* can be larger by an order of magnitude or more than ones in the infrared, which are mainly dependent on temperature structure. The data for microwave *Cn2* reported by Medeiros Filho et al. (1988) appear to agree quite well with this rule. Medeiros Filho et al. (1988) derived values for microwave *Cn2* from atmospheric temperature and humidity spectra information, which were collected on an instrumented mast above a 50 m building in an urban setting. Considering altitude scaling, i.e., $z^{-2/3}$ (nighttime) or $z^{-4/3}$ (daytime), their microwave *Cn2* data (which were in the range 10^{-15} to 10^{-13} $m^{-2/3}$) were quite plausibly 10^3 or more times larger than values for *Cn2* that might have been calculated for visible or infrared wavelengths along that elevated path. Finally, Medeiros Filho et al. (1988) found that the average temperature, temperature-humidity cross-correlation, and humidity contributions to *Cn2* (based on 17 daytime and nighttime cases) were 12%, 39%, and 49%, respectively. From this they concluded that (within the inertial sub-range) the main contribution to microwave *Cn2* is atmospheric humidity (e.g., water vapor pressure) while, at the same time, the cross-correlation term has a considerable influence and therefore should not be neglected. [Note Wesely (1976) provided one of the best earlier papers to discuss the combined effect of temperature and humidity fluctuations on refractive index.]

Based on the structure function formulations given by Tatarski (1971), a useful expression for *Cn2* can be written as,

$$C_n^2 = b\varepsilon^{-1/3} K_H \left(\frac{\partial n}{\partial z}\right)^2 , \quad (1)$$

where b is a constant, K_H is the exchange coefficient for turbulent heat diffusion, k is Karman's constant, ε is the turbulent kinetic energy dissipation rate, and $\partial n/\partial z$ is the partial derivative of the index of refraction (n). A list of symbols and constants are given in the appendix. Equation 1 is assumed valid for $|\vec{r}|$ in the inertial sub-range, where $|\vec{r}|$ is a turbulent eddy length scale between the inner (viscous-dissipation) and outer (energy producing) turbulent scales (Tatarski, 1971; Ochs and Hill, 1985). Numerous atmospheric surface layer models of this type have been developed for estimating the refractive index structure parameter, *Cn2*, especially for visible, near-infrared, and infrared wavelengths (e.g., Wesely and Alcarez, 1973; Davidson et al., 1981; Kunkel and Walters, 1983; Andreas, 1988; Miller and Ricklin, 1990; Rachele and Tunick, 1994; de Bruin et al., 1995; Thiermann et al., 1995; Frederickson et al., 2000; and Tunick, 1998, 2003). In contrast, quite a few other authors have reported on measurements and model calculations of microwave refractivity and *Cn2* in the boundary layer and troposphere (e.g., Cole et al., 1978; VanZandt et al., 1978; Burk, 1980; Morrissey et al., 1987; Medeiros Filho et al., 1988; d'Auria et al., 1993; and Hocking and Mu, 1997). Table 1 lists selected reports on microwave *Cn2* data collected in diverse microclimates. Table 2 lists selected reports on computer models to derive microwave refractivity and *Cn2* profile information in the boundary layer and troposphere. As an example, Burk (1980) shows modeled profiles for microwave *Cn2*, wherein the main influences on *Cn2* are due to moisture (figure 1). Similarly, Hocking and Mu (1997) show measured profiles for microwave *Cn2*, wherein the effects on *Cn2* due to moisture gradients are highlighted (figure 2).

Table 1. List of selected reports on microwave *Cn2* data in diverse microclimates.

Microclimate category / subcategory	**Data summary**	**Lead Scientists / Laboratory, Agency, and University Affiliations**
Rural – Agricultural, forests, rivers, and lakes		
Boulder Atmospheric Observatory, Erie, CO	C_n^2, radio wave, FM-CW boundary layer profiles	Gossard et al., (1984), CIRES, Univ. of Colorado
Meadows, grass-covered fields, and wooded areas, The Netherlands	C_n^2, radio wave, derived from a 30GHz (1 cm) radio link, LOS 8.2 km @ 44-77 m a.g.l.	Herben and Kohsiek (1984), Eindhoven Univ. of Technology and KNMI, The Netherlands
CASES-99 field site, grass-covered fields and wooded areas, Central Kansas	C_n^2, microwave, 915 MHz turbulent eddy profiler; C_n^2, radio-wave, 2.7 GHz FM-CW boundary layer radar	Ince et al., (2000) Univ. of Massachusetts, Amherst
Urban – City and residential buildings		
Above and in between city buildings, Central London	C_n^2, millimeter (110GHz); C_n^2, microwave (36 GHz), derived from log-amplitude fluctuation data, LOS 4.1 km @ 50 m a.g.l., on average	Cole et al., (1978) University College London, England
Above and in between city buildings, Central London	C_n^2, microwave, derived from wet- and dry-bulb temperature and wind data	Medeiros Filho et al., (1988) University College London, England
Coastal Areas		
Over barrier islands and along coastline, Chatham, MA	C_n^2, aircraft-mounted microwave refractometer, boundary layer optical turbulence data	Morrissey et al., (1987) Air Force Geophysics Laboratory, Hanscom, AFB
Over the continental and coastal regions of the Asiatic Arctic, Siberia	Radio-wave refractive index gradient data derived from radiosonde water vapor and temperature profile data	Darizhapov et al., (1988) Academy of Sciences, USSR
Southern California coastal region, Point Magu, CA	Radio-wave refractive index profiles derived from (uv/visible) Lidar and radiosonde retrieved water vapor and temperature data	Blood et al., (1994), Space and Naval Warfare Systems Command (SPAWAR) Systems Center, San Diego, CA
Southern California coastal region, Point Magu, CA	Radio-wave refractive index profiles derived from Ground-Based High Resolution Interferometer Sounder- and radiosonde-retrieved water vapor and temperature data	Wash and Davidson (1994) Space and Naval Warfare Systems Command (SPAWAR) Systems Center, San Diego, CA
Buckland Park VHF radar facility, Southern Australia	C_n^2, radio wave, 54.1 MHz (VHF) Doppler radar and thermosonde data	Hocking and Mu, (1997), Univ. of Western Ontario, Canada Univ. of Adelaide, Australia
Ocean – Tropical		
East of Singapore, close to the equator, South China Sea	Radio-wave refractive index gradient data derived from radiosonde water vapor and temperature profile data	Ong and Ong (2000) Nanyang Technical Univ., Republic of Singapore

Table 2. List of selected reports on computer models to derive microwave refractivity and *Cn2* profile information.

Range	**Model summary**	**Lead Scientists / Laboratory, Agency, or University**
5 km < h < 15 km a.g.l.	C_n^2 microwave; Radiosonde temperature, humidity, and wind speed data model; Includes formulations of Tatarski (1971) for the radio refractive index structure constant.	VanZandt et al., (1978) NOAA Aeronomy Laboratory, Boulder, CO
10 m < h < 2000 m a.g.l.	C_n^2 optical and microwave; Higher-order turbulence closure model; includes expressions for the temperature, and moisture structure parameters given by Wesley (1976).	Burk (1980) Naval Environmental Prediction Research Facility, Monterey, CA
100 m < h < 6000 m a.g.l.	C_n^2 microwave; Model for ground-based clear-air FM-CW Doppler radars; determines velocity variance, t.k.e. dissipation rate, and wind shear.	Gossard et al., (1982) NOAA Wave Propagation Laboratory, Boulder, CO
0.01 km < h < 20 km a.g.l.	C_n^2 optical, infrared, and microwave; –2/3, –4/3 power law profile expressions; additional empirical models based on tropospheric wind observations.	Good et al., (1988) Air Force Geophysical Laboratory, Hanscom AFB, MA
10 m < h < 4200 m a.g.l.	C_n^2 microwave; Radiosonde temperature, humidity, and wind speed model; includes formulations of Tatarski (1971); includes algorithm to calculate turbulence due to intermittency.	d'Auria et al., (1993) University of Rome, Italy
10 m < h < 1200 m a.g.l.	C_n^2 microwave; 4D refractivity field forecast model;.temperature, wind speed, and humidity gradients derived from Navy hydrostatic mesoscale numerical model.	Burk and Thompson (1997) Naval Research Laboratory, Monterey, CA
10 m < h < 2000 m a.g.l.	C_n^2 microwave; 3D time-dependent fields of turbulent refractivity calculated using a large eddy simulation (LES) model for the daytime boundary layer, convective case.	Gilbert et al., (1999) National Center for Physical Acoustics Univ. of Mississippi, MS
10 m < h < 1200 m a.g.l.	C_n^2 microwave; 4D refractivity field forecast model; Temperature, wind speed, and humidity gradients derived from the UK Meteorological Office, non-hydrostatic, mesoscale numerical model	Atkinson et al., (2001) University of London, UK

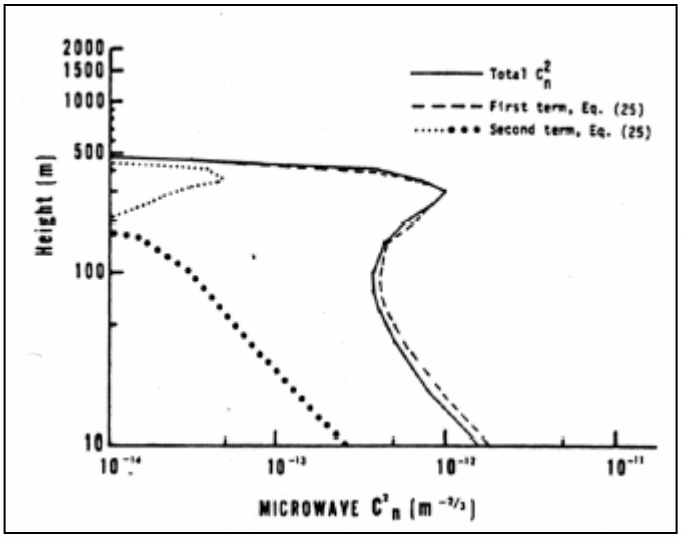

Figure 1. Modeled profiles of microwave *Cn2* over oceans (from Burk, 1980).

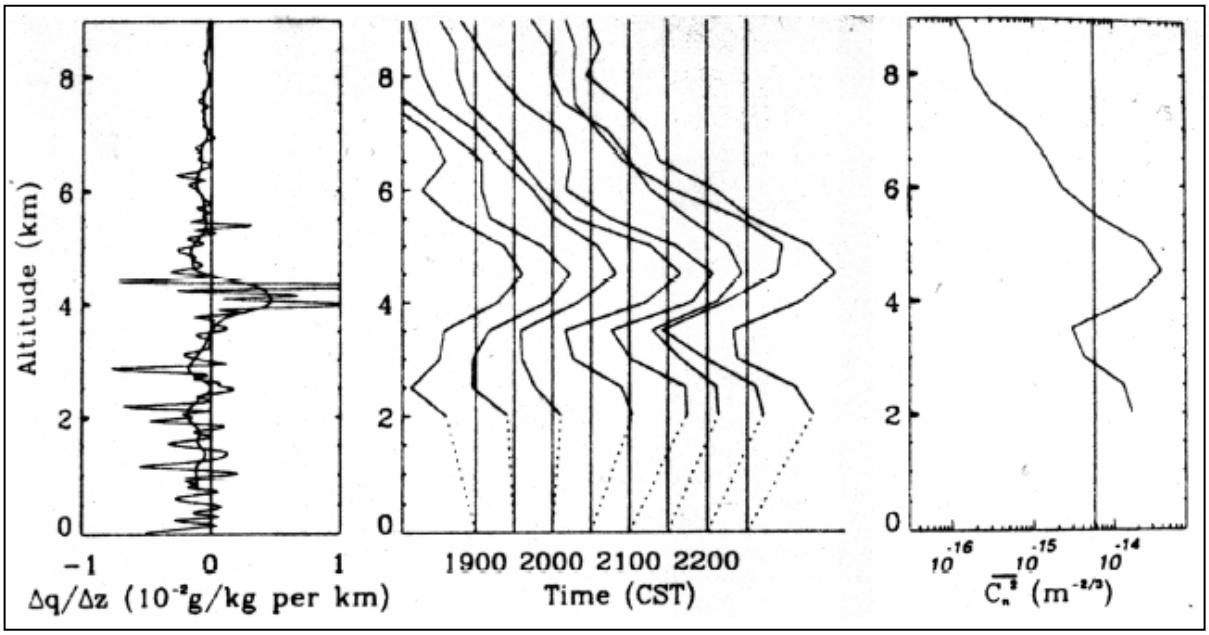

Figure 2. Measured profiles of microwave *Cn2* and the humidity gradient over Adelaide, Australia, collected at the Buckland Park (54.1 MHz) Radar Facility. The vertical lines are centered at $\log_{10} Cn2 = -14.25$ (from Hocking and Mu, 1997).

3. Computational Algorithms

The refractive index in air (n) can be expressed in terms of air density (i.e., pressure, temperature, and water vapor content). The following equations are expressions for the real index of refraction in air as reported by Andreas (1988), who references Owens (1967), for visible and near-infrared regions. Andreas' formulations, which are expressed in terms of air temperature, T, and absolute humidity, Q, alternatively can be given in terms of the conserved variables potential temperature (θ) and specific humidity (q). Absolute humidity expressed as $Q = \frac{100.}{R_v}\frac{e}{T}$ where $R_v = 461.50\ J\ Kg^{-1}K^{-1}$ is the gas constant for water vapor and vapor pressure, as shown in Hess (1979), given as $e \approx 0.622Pq$, combine to yield the expression $Q = 0.348\frac{Pq}{T}$.

Within visible and near-infrared regions from 0.36 to 3 μm (as indicated by the subscript v), the real index of refraction in air can be written as,

$$n_v = 1 + \left(M_1(\lambda)\frac{P}{T} + 1.61\ (M_2(\lambda) - M_1(\lambda))\frac{Pq}{T} \right) x\,10^{-6}, \qquad (2)$$

which are basically the first order terms of the refractivity (dispersion) and density formulas for dry air, water vapor, and carbon dioxide (Owens, 1967) as a function of wavelength (λ), where

$$M_1(\lambda) = 23.7134 + \frac{6839.397}{130 - \sigma^2} + \frac{45.473}{38.9 - \sigma^2}\ , \qquad (3)$$

and

$$M_2(\lambda) = 64.8731 + 0.58058\,\sigma^2 - 0.007115\,\sigma^4 + 0.0008851\,\sigma^6\ , \qquad (4)$$

where $\sigma = \lambda^{-1}$ (wavelength^{-1}). Assuming steady state, homogeneous conditions, and considering the pressure partial derivative (in the surface layer) to be negligible, then taking the partial derivative of equation 2 yields,

$$\frac{\partial n_v}{\partial z} = \left(-M_1(\lambda)\frac{P}{T^2} - 1.61(M_2(\lambda) - M_1(\lambda))\frac{Pq}{T^2} \right) x\,10^{-6}\frac{\partial \theta}{\partial z} \qquad (5)$$

$$+ 1.61(M_2(\lambda) - M_1(\lambda))\frac{P}{T}\,x\,10^{-6}\frac{\partial q}{\partial z}$$

In the lower atmosphere (z < 10 km) the potential temperature (θ) and moisture (q) partial derivatives $\partial\theta/\partial z$ and $\partial q/\partial z$, can be calculated from atmospheric data via instrumented radio-sondes (e.g., d'Auria et al., 1993; Vasseur, 1999). Similar expressions for the partial derivative of the refractive index can be derived for infrared (7.8 to 19 μm), near-millimeter (0.3 to 3 mm) and microwave (radio) wavelengths (reference Andreas, 1988), as had been shown, for example, in the paper given by Tunick and Rachele (1991).

For infrared (IR) wavelengths from 7.8 to 19 μm (as indicated by the subscript i) the real index of refraction in air can be written as described by Hill and Lawrence (1986) and Owens (1967), as

$$n_i = 1 + \left(n_v^d + n_i^w\right)\times 10^{-6} \tag{6}$$

where in the range –40 to +40 ºC,

$$n_i^w = Q\left[\frac{957. - 928.\alpha^{0.4}(X-1)}{1.03\alpha^{0.17} - 19.8X^2 + 8.2X^4 - 1.7X^8} + \frac{3.747\times 10^6}{12499. - X^2}\right], \tag{7}$$

and

$$n_v^d = \left(M_1(\lambda)\frac{P}{T} - 4.615\,M_1(\lambda)Q\right) \tag{8}$$

where $X = \frac{10\mu m}{\lambda}$, and $\alpha = \frac{T}{273.15}$.

$$\frac{\partial n_i}{\partial z} = \left(-M_i(\lambda)\frac{P}{T^2} + 1.6095M_i(\lambda)\frac{Pq}{T^2} + 0.34875\frac{Pq}{T}[A] - 0.34875[B]\frac{Pq}{T^2}\right)\times 10^{-6}\frac{\partial\theta}{\partial z} \tag{9}$$

$$+\left(0.34875[B] - 1.6095M_1(\lambda)\right)\frac{P}{T}\times 10^{-6}\frac{\partial q}{\partial z}$$

where

$$[A] = \left(-\frac{1.359\alpha^{-0.6}(X-1)}{1.03\alpha^{0.17} - 19.8X^2 + 8.2X^4 - 1.7X^8} + \frac{0.5949\alpha^{0.43}(X-1)}{\left(1.03\alpha^{0.17} - 19.8X^2 + 8.2X^4 - 1.7X^8\right)^2}\right) \tag{10}$$

and

$$[B] = \left[\frac{957. - 928.\alpha^{0.4}(X-1)}{1.03\alpha^{0.17} - 19.8X^2 + 8.2X^4 - 1.7X^8} + \frac{3.747\times 10^6}{12499. - X^2}\right]. \tag{11}$$

For the radio region (wavelengths greater than 3 mm) as indicated by the subscript *r*, Andreas (1988) provides the following expression for the refractive index, i.e.,

$$n_r = 1 + \left(n_{rd} + n_{rw}\right) \times 10^{-6} \quad , \tag{12}$$

where, from Hill et al. (1982) and Boudouris (1963),

$$n_{rd} = 77.6 \frac{(P - e)}{T} \quad , \tag{13}$$

and

$$n_{rw} = 72.0 \frac{e}{T} + 0.375 \times 10^6 \frac{e}{T^2} \quad , \tag{14}$$

where e (vapor pressure) = 4.615 QT. Since, $Q = 0.34875 \frac{Pq}{T}$ (for P in millibars) then $e = 1.6096 Pq$. Substituting this expression for vapor pressure (e) into equations 13 and 14 yields,

$$n_{rd} = 77.6 \frac{P}{T} - 1.249 \times 10^2 \frac{Pq}{T} \quad , \tag{15}$$

and

$$n_{rw} = 1.159 \times 10^2 \frac{Pq}{T} + 6.0356 \times 10^5 \frac{Pq}{T^2} \quad . \tag{16}$$

Now, from equations 12, 15, and 16 we obtain

$$\begin{aligned} \frac{\partial n_r}{\partial z} = & \left(-77.6 \frac{P}{T^2} + 9.0 \frac{Pq}{T^2} - 1.2071 \times 10^6 \frac{Pq}{T^3} \right) \times 10^{-6} \frac{\partial \theta}{\partial z} \\ & + \left(-9.0 \frac{P}{T} + 6.0356 \times 10^5 \frac{P}{T^2} \right) \times 10^{-6} \frac{\partial q}{\partial z} \end{aligned} \quad . \tag{17}$$

For the near-millimeter region (wavelengths from 0.3 to 3 mm) as indicated by the subscript *m*, Andreas (1988) provides the following expression for the refractive index, i.e.,

$$n_m = 1 + \left(n_{rd} + n_{rw} + n_{mw1} + n_{mw2}\right) \times 10^{-6} \tag{18}$$

where n_{rd} and n_{rw} are given above, n_{mw1} is due to vapor resonances at wavelengths < 0.3 mm, and n_{mw2} is due to water-vapor resonances at wavelengths > 0.3 mm. According to Andreas (1988), Hill (1988) evaluated the n_{mw1} and n_{mw2} terms, and although the n_{mw2} term requires a line-by-line summation of the resonances and consequently does not have a single analytical form, he did produce an approximation for n_{mw1}, i.e.,

$$n_{mw1} = Q \sum_{j=1}^{4} \alpha_j (296/T)^{a_j} \left[1 - B_j (296/T)\right](0.303/\lambda)^{2j} \quad , \tag{19}$$

where α_j, a_j, and B_j are given in table 3.

Table 3. The coefficients in equation 19.

j	α_j	a_j	B_j
1	1.388221 x 10^3	1.650	0.1993324
2	-0.2135129 x 10^3	0.1619430	3.353494
3	-0.1485997 x 10^3	0.1782352	3.100942
4	-0.1088790 x 10^3	0.1918662	3.004944

For the sake of an analytic solution, Andreas (1988) does not consider the effect of n_{mw2}. We follow his lead in our formulation. As such the approximation should be accurate to ± 10% in the window regions 0.31 – 0.34 mm (880 – 970 GHz), 0.42 – 0.44 mm (680 – 720 GHz), and 0.83 – 3.0 mm (100 – 360 GHz).

Rewriting equation 19 in terms of specific humidity (q) gives,

$$n_{mw1} = 0.34875 \frac{Pq}{T} \sum\left(\quad \right) \quad . \tag{20}$$

The contribution of equation 20 to $\frac{\partial n_m}{\partial z}$ is

$$\frac{\partial n_m}{\partial z} = -0.34875 \frac{Pq}{T^2} \sum\left(\quad \right) \times 10^{-6} \frac{\partial \theta}{\partial z} + 0.34875 \frac{Pq}{T} \sum\left(\quad \right) \times 10^{-6} \frac{\partial q}{\partial z} \quad . \tag{21}$$

Finally, combining equations 18 and 21 yields,

$$\begin{aligned} \frac{\partial n_r}{\partial z} = & \left(-77.6 \frac{P}{T^2} + 9.0 \frac{Pq}{T^2} - 1.2071 \times 10^6 \frac{Pq}{T^3} - 0.34875 \frac{Pq}{T^2} \sum\left(\quad \right) \right) \times 10^{-6} \frac{\partial \theta}{\partial z} \\ & + \left(-9.0 \frac{P}{T} + 6.0356 \times 10^5 \frac{P}{T^2} + 0.34875 \frac{Pq}{T} \sum\left(\quad \right) \right) \times 10^{-6} \frac{\partial q}{\partial z} \end{aligned} \quad . \tag{22}$$

4. Summary and Conclusions

Optical turbulence is important because it can significantly degrade the performance of electro-magnetic systems and sensors, such as laser and microwave ground to satellite communications and infrared imaging. For example, changes in the refractive index of air along the transmission path can influence the temporal intensities of microwaves causing signal fades and surges. Changes in the refractive index or air can also cause wave-fronts to distort and change direction from their original path. This may lead to a significant increase in bit-error rates for communication downlinks or lead to system unavailability. While an earlier paper (Tunick, 2002) mainly described data and models associated with optical sensors, e.g., those aligned horizontally over various paths close to the ground, this paper focused instead on data and models for microwave *Cn2* through the boundary layer and troposphere. We have highlighted the importance of humidity effects on microwave *Cn2* and have presented a comprehensive reference list for selected past research on this topic of interest. We anticipate that our report will be of interest to scientists and engineers concerned with the design and performance of earth and space communication systems.

Literature Cited

Andreas, Edgar L, Estimating C_n^2 Over Snow and Sea Ice From Meteorological Data. *J. Opt. Soc. Amer*. **1988**, *5*, 481–495.

Atkinson, B. W.; Li, J-G Li; Plant, R. S. Numerical Modeling of the Propagation Environment in the Atmospheric Boundary Layer over the Persian Gulf. *J. Appl. Meteor.* **2001**, *40*, 586–603.

Beland R. R. Propagation Through Atmospheric Turbulence in The Infrared Electro-Optical Systems Handbook, J. S. Accetta and D. L. Shumaker (Eds), SPIE Press Monograph, PM10, Bellingham, WA, 1993.

Blood, D. W.; McKinley, S.; Philbrick, C. R.; Paulus, R.; Rodgers, T. Lidar Measured Refractive Effects in a Coastal Environment. In Proc., *International Geoscience and Remote Sensing Symposium (IGARSS'94)*, California Institute of Technology, Pasadena, CA, 1994.

Bohlander R. A.; McMillian, R. W.; Gallagher, J. J. Atmospheric Effects on Near-Millimeter Wave Propagation. *Proceedings of the IEEE*, 1985, 73, 49–60.

Boudouris, C. On the Index of Refraction of Air, the Absorption and Dispersion of Centimeter Waves by Gases. *Journal of Research at the National Bureau of Standards*, 1963, Sec. D, 63l–684.

Burk, S. D. Refractive Index Structure Parameters: Time-Dependent Calculations Using a Numerical Boundary-Layer Model. *J. Appl. Meteor.* **1980**, *19*, 562–576.

Burk, S. D.; Thompson, W. T. Mesoscale Modeling of Summertime Refractive Conditions in the Southern California Bight. *J. Appl. Meteor.* **1997**, *36*, 23–31.

Chiba, T. Spot Dancing of the Laser Beam Propagated Through the Turbulent Atmosphere. *Appl. Opt.* **1971**, *10*, 2456–2461.

Cole, R. S.; Ho, K. L.; Mavrokoukoulakis, N. D. The Effect of the Outer Scale of Turbulence and Wavelength on Scintillation Fading at Millimeter Wavelengths. *IEEE Trans. Antennas Propagat,* **1978**, *AP-26*, 712–715.

d'Auria, G.; Marzano, F. S.; Merlo, U. Model for Estimating the Refractive-Index Sructure Constant in Clear-Air Intermittent Turbulence. *Appl. Opt*. **1993**, *32*, 2674–2680.

Darizhapov, D. D.; Zhamsuyeva, G. S.; Chimitdorzhiyev, N. B. Variations in the Vertical Gradient of the Index of Refraction in the Polar Troposphere. *Izvestiya, Atmospheric and Oceanic Physics* **1988**, *24*, 714–718.

Davidson, K. L.; Schacher, G. E.; Fairall, C. W.; Goroch, A. K. Verification of the Bulk Model for Calculating Overwater Optical Turbulence. *Appl. Opt*. **1981**, *20*, 2929–2924.

de Bruin, H.A.R.; van den Hurk, B.J.J.M.; Kohsiek, W. The Scintillation Method Tested Over a Dry Vineyard Area. *Bound-Layer Meteor.* **1995**, *76,* 25–40.

Frederickson, P. A.; Davidson, K. L.; Zeisse, C. R.; Bendall, C.S. Estimating the Refractive Index Structure Parameter (CN2) Over the Ocean Using Bulk Methods. *J. App. Meteorol.* **2000**, *39*, 1770–1783.

Fried, D. L.; Mevers, G. E.; Keister, M. P. Measurements of Laser Beam Scintillation in the Atmosphere. *J. Opt. Soc. Am.* **1967**, *57*, 787–797.

Gilbert, K. E.; Di, X.; Khanna, S.; Otte, M. J.; Wyngaard, J. C. Electromagnetic Wave Propagation Through Simulated Atmospheric Refractivity. *Radio Sci.* **1999**, *34*, 1413–1432.

Good, R. E.; Beland, R. R.; Murphy, E. A.; Brown, J. H.; Dewan, E. M. Atmospheric Models of Optical Turbulence. In *Modeling of the Atmosphere*, Proc. 1988, SPIE 928, 165–186.

Gossard, E. E.; Chadwick, R. B.; Neff, W. D.; Moran, K. P. The Use of Ground-Based Doppler Radars to Measure Gradients, Fluxes, and Structure Parameters in Elevated Layers. *J. Appl. Meteor* **1982**, *21*, 211–226.

Gossard, E. E.; Chadwick, R. B.; Detman, T. R.; Gaynor, J. Capability of Surface-Based Clear-Sir Doppler Tadar for Monitoring Meteorological Dtructure of Rlevated Layers. *J. Climate and Appl. Meteor* **1984**, *23*, 474–485.

Herben, M.H.A.J.; Kohsiek, W. A Comparison of Radio Wave and in situ Observations of Tropospheric Turbulence and Wind Velocity. *Radio Sci.* **1984**, *19*, 1057–1068.

Hess, S. L., *Introduction to Theoretical Meteorology*. Robert E. Krieger Publishing Co., Huntington, NY, 362 pp 1979.

Hill, R. J. Dispersion by Atmospheric Water Vapor at Frequencies Less Than 1 THz. *IEEE Transactions on Antennas and Propagation* **1988**, *36*, 423–430.

Hill, R. J.; and Lawrence, R. S. Refractive Index of Water Vapor in Infrared Windows. *Infrared Physics* **1986**, *26*, 371–376.

Hill, R. J.; Lawrence, R. S.; Priestley, J. T. Theoretical and Calculational Aspects of the Radio Refractive Index of Water Vapor. *Radio Sci.* **1982**, *17*, l251–1257.

Hocking, W. K.; Mu, P.K.L. Upper and Middle Tropospheric Kinetic Energy Dissipation Rates From Measurements of Cn2 – Review of Theories, *in-situ* Investigations, and Experimental Studies Using the Buckland Park Atmospheric Radar in Australia. *J. Atmos. and Solar-Terrestrial Phys.* **1997**, *59*, 1779–1803.

Ince, T.; Li, J.; Lopez-Dekker, F.; Pazmany, A. L.; Frasier, S. J. Radar Observations of Stable Boundary Layer During CASES'99. In Proc., *14th Symp on Boundary Layers & Turbulence*, Amer. Meteor. Soc., 2000, Boston, MA.

Ishimaru, A. The Beam Wave Case and Remote Sensing. in *Laser Beam Propagation in the Atmosphere*, J. W. Stronbehn (Ed.), Springer-Verlag, New York, 1978, 129–170.

Kallistratova, M. A.; Timanovskiy, D. F. The Distribution of the Structure Constant of Fefractive Index Fluctuations in the Atmospheric Surface Layer. *Izv. Acad. Sci. USSR Atmos. Oceanic Phys., Engl. Transl*. **1971**, *7*, 46–48.

Kopeika N. S. *A System Engineering Approach to Imaging*. Bellingham, WA: SPIE Optical Engineering Press, 1998, 679 pp.

Kunkel, K. E.; Walters, D. L. Modeling the Diurnal Dependence of the Optical Refractive Index Structure Parameter. *J. Geophys. Res.* **1983**, *88*, 10999–11004.

Medeiros Filho, F. C.; Jayasuriya, D.A.R.; Cole, R. S.; Helmis, C. G.; Asimakopoulos, D. N. Correlated Humidity and Yemperature Measurements in the Urban Boundary Layer. *Meteorol. Atmos. Phys.* **1988**, *39*, 197–202.

Miller, W. B.; Ricklin, J. C. *A Module for Imaging Through Optical Turbulence: IMTURB*; ASL-TR-0221-27; Army Research Laboratory: Adelphi, MD, 1990.

Morrissey, J. F.; Izumi, Y.; Cote, O. R. *Microwave Refractive Iindex Structure Function Profiles (C_n^2) measured from small aircraft*; AFGL-TR-87-008; Air Force Geophysics Lab: Hanscom, AFB, MA, 1987.

Ochs, G. R. and Hill, R. J. Optical-Scintillation Method for Measuring Turbulence Inner-Scale. *Appl. Opt.* **1985**, *24*, 2430–2432.

Ong, S-F.; Ong, J-T. Studies on the Refractive Index Structure in Singapore. In Proc., *Antennas and Propagation Society International Symposium, IEEE* **2000**, *4*, 2099–2102.

Owens, J. C. Optical Refractive Index of Air; Dependence on Pressure Temperature and Composition. *Appl.Opt.* **1967**, *6***,** 51–59.

Parry, G. Measurement of Atmospheric Turbulence Induced Intensity Fluctuation in a Laser Beam. *Opt. Acta (J. Modern Opt*.) **1981**, *28*, 715–728.

Rachele, H.; Tunick, A. Energy Balance Model for Imagery and Electromagnetic Propagation. *J. Appl. Meteor.* **1994**, *33*, 964–976.

Tatarski, V. I. *The Effects of the Turbulent Atmosphere on Wave Propagation, Israel Program for Scientific Translations*, Jerusalem, 472 pp. (available as NTIS Technical Translation 68-50464) 1971.

Thiermann, V.; Karipot, A.; Dirmhirn, I.; Poschl, P.; Czekits, C. Optical Turbulence Over Paved Surfaces. In Proc., *Atmospheric Propagation and Remote Sensing IV*, 1995, SPIE vol. 2471, J.C. Dainty (Ed.) 197–203.

Tunick, A. *The Refractive Index Structure Parameter/Atmospheric Optical Turbulence Model:CN2*; ARL-TR-1615; U.S. Army Research Laboratory: Adelphi, MD, 1998.

Tunick, A. *A Critical Assessment of Selected Past Research on Optical Turbulence Information in Diverse Microclimates*; ARL-MR-521; U.S. Army Research Laboratory: Adelphi, MD, 2002.

Tunick, A. CN2 Model to Calculate the Micrometeorological Influences on the Refractive Index Structure Parameter. *Environ. Modell. Softw.* **2003**, *18* (2), 165–171.

Tunick, A. Toward Increasing the Accuracy and Realism of Future Optical Turbulence (Cn2) calculations. *Meteorol. Atmos. Phys.* **2005**, *90*, 159–164.

Tunick, A.; Rachele, H. Estimating Effects of Temperature and Moisture on Cn2 in the Damp Unstable Boundary Layer for Visible, Infrared, Radio, and Millimeter Wavelengths. In *Atmospherics Propagation and Remote Sensing, Proc. SPIE*, 1992, 1688.

VanZandt, T. E.; Green, J. L.; Gage, K. S.; Clark W. L. Vertical Profiles of Refractivity Turbulence Structure Constant: Comparison of Observations by Sunset radar with a New Theoretical Model. *Radio Sci.* **1978**, *13*, 819–829

Vander Vorst A.; Vasseur, H.; Vyncke, C.; Byrne, C. A.; Vanhoenacker-Janvier, D. From Electromagnetics to System Performance: A New Method for the Error-Rate Prediction of Atmospheric Communication Links. *IEEE Journal on Selected Areas in Communications* **1997**, *15*, 656–666.

Vasseur H. Prediction of Tropospheric Scintillation on Satellite Links From Radiosonde Data. *IEEE Transactions on Antennas and Propagation* **1999**, *47*, 293–301.

Wash, C. H.; Davidson, K. L. Remote Measurements and Coastal Atmospheric Refraction. In Proc., *International Geoscience and Remote Sensing Symposium (IGARSS'94)*, California Institute of Technology: Pasadena, CA, 1994.

Wesely, M. L.; Alcarez, E. C. Diurnal Cycles of the Refractive Index structure Function Coefficient. *J. Geophys. Res*. **1973**, *78*, 6224–6232.

Wesely, M. L. The Combined Effect of Temperature and Humidity Fluctuations on Refractive Index. *J. Appl. Meteor*. **1976**, *15*, 43–49.

Wilson, K. E.; Lesh, J. R.; Araki, K., Arimoto, Y. Overview of the Ground-to-Orbit Lasercom Demonstration (GOLD). In Proc., *Free-Space Laser Communication Technologies IX*, SPIE, vol. 2990, G. Stephen Mecherle (Ed.), 1997, 23–30.

INTENTIONALLY LEFT BLANK.

Appendix – List of Symbols and Constants

Symbol	Name or Description
a_j	Coefficient in equation 19 given in table 3.
B	Obukhov-Corrsin constant
B_j	Coefficient in equation 19 given in table 3.
Cn2 or C_n^2	Refractive index structure parameter
e	Water vapor pressure
K_H	Turbulent eddy exchange coefficient for heat
LOS	Line of sight
$M_1(\lambda)$	Constant in equations 2 and 5
$M_2(\lambda)$	Constant in equations 2 and 5
n	Index of refraction
n_i	Index of refraction (infrared wavelengths)
n_i^w	Refractivity due to water vapor (infrared wavelengths)
n_m	Index of refraction (near-millimeter wavelengths)
n_{mw1}	Refractivity due to water-vapor resonances at wavelengths < 0.3 mm
n_{mw2}	Refractivity due to water-vapor resonances at wavelengths > 0.3 mm.
n_r	Index of refraction (radio wavelengths)
n_{rd}	Contribution from dry air to the instantaneous refractivity (radio wavelengths)
n_{rw}	Refractivity due to water vapor (radio wavelengths)
n_v	Index of refraction (visible wavelengths)
n_v^d	Contribution from dry air to the instantaneous refractivity (visible wavelengths)
P	Atmospheric pressure in millibars
q	Specific humidity in kg/kg
Q	Absolute humidity in kg/m^3

$\lvert\vec{r}\rvert$	Turbulent eddy length scale between the inner (viscous-dissipation) and outer (energy producing) turbulent scales
R_v	Gas constant for water vapor
T	Air temperature in Kelvin
X	Scaled wavelength
Z	Height in meters above ground
α	Scaled temperature
α_j	Coefficient in equation 19 given in table 3.
ε	Energy dissipation rate
λ	Wavelength in μm
θ	Potential temperature
σ	$\frac{1}{wavelength}$
$\left\langle \sigma_A^2 \right\rangle$	Angle of arrival fluctuation variance
$\left\langle \sigma_x^2 \right\rangle$	Log-intensity (long-amplitude) variance of transmitted electromagnetic signals
$\frac{\partial \theta}{\partial z}$	Vertical gradient of potential temperature
$\frac{\partial q}{\partial z}$	Vertical gradient of specific humidity
$[A]$, $[B]$	Placement variables in equation 9
$\partial n / \partial z$	Vertical gradient of the index of refraction
$\frac{\partial n_i}{\partial z}$	Vertical gradient of the index of refraction (infrared wavelengths)
$\frac{\partial n_m}{\partial z}$	Vertical gradient of the index of refraction (near-millimeter wavelengths)

$\frac{\partial n_r}{\partial z}$ Vertical gradient of the index of refraction (radio wavelengths)

$\frac{\partial n_v}{\partial z}$ Vertical gradient of the index of refraction (visible wavelengths)

INTENTIONALLY LEFT BLANK

Distribution List

ADMNSTR
DEFNS TECHL INFO CTR
ATTN DTIC-OCP (ELECTRONIC COPY)
8725 JOHN J KINGMAN RD STE 0944
FT BELVOIR VA 22060-6218

DARPA
ATTN IXO S WELBY
3701 N FAIRFAX DR
ARLINGTON VA 22203-1714

SCI & TECHNLGY CORP
10 BASIL SAWYER DR
HAMPTON VA 23666-1293

US ARMY CRREL
ATTN CERCL-SI E L ANDREAS
72 LYME RD
HANOVER NJ 03755-1290

NAV POSTGRADUATE SCHL
DEPT OF METEOROLOGY
ATTN P FREDERICKSON
1 UNIVERSITY CIR
MONTEREY CA 93943-5001

AIR FORCE
ATTN WEATHER TECHL LIB
151 PATTON AVE RM 120
ASHEVILLE NC 28801-5002

COLORADO STATE UNIV
DEPT OF ATMOS SCI
ATTN R A PIELKE
200 WEST LAKE STREET
FT COLLINS CO 80523-1371

THE CITY COLLEGE OF NEW YORK
DEPT OF EARTH & ATMOS SCI
ATTN S D GEDZELMAN
J106 MARSHAK BLDG 137TH AND
CONVENT AVE
NEW YORK CITY NY 10031

UNIV OF ALABAMA AT HUNTSVILLE
DEPT OF ATMOS SCI
ATTN R T MCNIDER
HUNTSVILLE AL 35899

NATL CTR FOR ATMOS RSRCH
ATTN NCAR LIBRARY SERIALS
PO BOX 3000
BOULDER CO 80307-3000

US ARMY RSRCH LAB
ATTN AMSRD-ARL-CI-OK-TP TECHL
LIB T LANDFRIED (2 COPIES)
ABERDEEN PROVING GROUND MD
21005-5066

DIRECTOR
US ARMY RSRCH LAB
ATTN AMSRD-ARL-RO-EV W D BACH
PO BOX 12211
RESEARCH TRIANGLE PARK NC 27709

US ARMY RSRCH LAB
ATTN AMSRD-ARL-CI J GOWENS
ATTN AMSRD-ARL-CI-C L TOKARCIK
ATTN AMSRD-ARL-CI-C
M VORONTSOV
ATTN AMSRD-ARL-CI-C B BROOME

ATTN AMSRD-ARL-CI-CN A TUNICK
(12 COPIES)
ATTN AMSRD-ARL-CI-CN
G CARHART
ATTN AMSRD-ARL-CI-CN G RACINE
ATTN AMSRD-ARL-CI-CS K DEACON
ATTN AMSRD-ARL-CI-CS R MEYERS
ATTN AMSRD-ARL-CI-OK-T
TECHL PUB (2 COPIES)
ATTN AMSRD-ARL-CI-OK-TL
TECHL LIB (2 COPIES)
ATTN AMSRD-ARL-D J M MILLER
ATTN AMSRD-ARL-D J ROCCHIO
ATTN IMNE-ALC-IMS MAIL &
RECORDS MGMT
ADELPHI MD 20783-1197